Development 133, 3283-3293 (2006) doi:10.1242/dev.02468

Cooperative activities of *Drosophila* DE-Cadherin and DN-Cadherin regulate the cell motility process of ommatidial rotation

Ivana Mirkovic and Marek Mlodzik*

Ommatidial rotation is a cell motility read-out of planar cell polarity (PCP) signaling in the *Drosophila* eye. Although the signaling aspects of PCP establishment are beginning to be unraveled, the mechanistic aspects of the associated ommatidial rotation process remain unknown. Here, we demonstrate that the *Drosophila* DE- and DN-cadherins have opposing effects on rotation. DE-cadherin promotes rotation, as DE-cad mutant ommatidia rotate less than wild type or not at all. By contrast, the two DN-cadherins act to restrict this movement, with ommatidia rotating too fast in the mutants. The opposing effects of DE- and DN-cadherins result in a coordinated cellular movement, enabling ommatidia of the same stage to rotate simultaneously. Genetic interactions, phenotypic analysis and localization studies indicate that EGF-receptor and Frizzled-PCP signaling feed into the regulation of cadherin activity and localization in this context. Thus, DE- and DN-cadherins integrate inputs from at least two signaling pathways, resulting in a coordinated cell movement. A similar input into mammalian E- and N-cadherins might function in the progression of diseases such as metastatic ovarian cancer.

KEY WORDS: *Drosophila*, Cadherins, Cell motility

INTRODUCTION

Cell polarization is essential for cellular function, patterning and cytoskeletal organization. Epithelial cells are polarized along the apicobasal axis. In addition, many tissues are polarized within the plane of the epithelium, generally called planar cell polarity (PCP). The conserved signaling events that regulate PCP are mediated by the Frizzled (Fz) pathway (Adler, 2002; Klein and Mlodzik, 2005; Mlodzik, 2002; Shulman et al., 1998; Veeman et al., 2003). Although genetic screens have identified many signaling molecules that participate in PCP signaling, the relationship between signaling events and changes in cytoskeletal organization and/or cellular adhesion remains unclear.

The read-out of PCP signaling is often the organization of cytoskeletal elements or orientation of the mitotic spindle (Adler, 2002; Bellaiche et al., 2001; Klein and Mlodzik, 2005; Shulman et al., 1998). PCP is also evident in neural sensory epithelia, most prominently in the *Drosophila* eye (Mlodzik, 1999; Strutt and Strutt, 1999) and mammalian inner ear (Dabdoub et al., 2003; Montcouquiol et al., 2003). In the *Drosophila* eye, PCP establishment includes transcriptional events linked to photoreceptor cell fate specification and complex cellular movements that cause ommatidial precursors to undergo a 90° rotation towards the midline of the developing eye field (Mlodzik, 1999; Strutt and Strutt, 1999).

Drosophila eyes are composed of ~800 ommatidia, each consisting of eight photoreceptor cells, and 12 accessory cells. Ommatidial assembly begins posterior to an organizing center, the morphogenetic furrow (MF), an indentation that forms at the posterior of the eye disc and moves across the developing disc. Photoreceptor precursors are assembled and specified behind the MF in a stereotyped manner, with R8 being the first, followed by pair-wise recruitment of R2/R5, R3/R4 and R1/R6, and finally R7 (Wolff and Ready, 1993).

Correct R3/R4 specification is crucial for PCP establishment. Initially, this photoreceptor pair is symmetrical. Then, the cell located closer to the dorsoventral (D/V) midline, the equator, receives a higher level of Fz signal, which specifies it as R3, and causes a transcriptional upregulation of *Delta* in the same cell. Delta then activates Notch signaling in the neighboring cell of the pair, specifying it as R4 (Cooper and Bray, 1999; Fanto and Mlodzik, 1999; Tomlinson and Struhl, 1999). As a result of distinct R3/R4 specification, ommatidial preclusters lose their symmetry and adopt two opposing mirror-image chiral forms in the ventral and dorsal eye hemispheres (Mlodzik, 1999; Strutt and Strutt, 1999).

Following R3/R4 specification, ommatidial preclusters rotate towards the equator (Mlodzik, 1999; Strutt and Strutt, 1999; Wolff and Ready, 1993). Each cluster rotates as a unit; this process is highly coordinated as clusters of the same maturity rotate simultaneously. At its end, ommatidia have rotated 90° away from their original position. R3/R4 specification is a prerequisite for the correct direction of rotation, resulting in dorsal and ventral ommatidia rotating in opposite directions (Mlodzik, 1999; Strutt and Strutt, 1999). Both the establishment of asymmetry within nascent ommatidial clusters and the subsequent rotation event lead to the final ommatidial arrangement, reflected in the mirror-image symmetry across the equator (Fig. 1).

How ommatidial rotation initiates is unknown. The signal to stop rotation at 90° is also unknown, but likely involves EGF-receptor (Egfr) and Notch (N) signaling (Brown and Freeman, 2003; Chou and Chien, 2002; Gaengel and Mlodzik, 2003; Strutt and Strutt, 2003). Fz/PCP signaling may regulate rotation through effects on cytoskeletal elements and cell-adhesion molecules. This is supported by the observation that *rok* (*Drosophila* Rho-associated kinase), an effector of the RhoA GTPase that has been placed genetically downstream of Fz has a rotation-specific eye phenotype (Winter et al., 2001). Finally, based on genetic evidence, initiation of the second

Brookdale Department of Molecular, Cell and Developmental Biology, Mount Sinai School of Medicine, New York, NY, USA.

*Author for correspondence (e-mail: marek.mlodzik@mssm.edu)

Accepted 1 June 2006

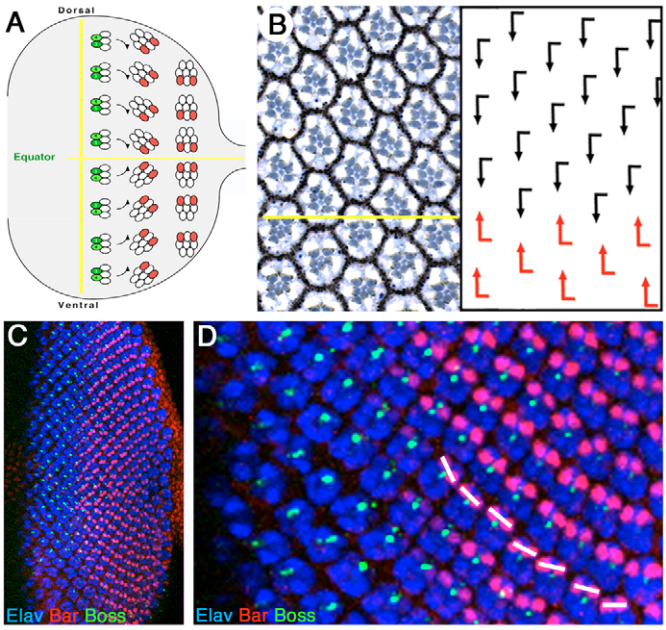

Fig. 1. Ommatidial rotation during PCP establishment in *Drosophila* eye. (**A**) Schematic presentation of ommatidial rotation in 3rd instar larval eye disc. Photoreceptors differentiate behind the morphogenetic furrow (MF, vertical yellow line). Five-cell preclusters are first organized in the AP axis. As photoreceptors become specified in the precluster, the group of cells simultaneously undergoes a 90° rotation towards the equator (horizontal yellow line). Green cells highlight R3/R4 precursors, and red marks future R1/R6 (stained with anti-Bar in C,D). (**B**) Tangential section of adult eye with ommatidia having completed 90° rotation (equator: yellow line). Right panel shows schematic presentation with dorsal and ventral chiral forms indicated with black and red arrows, respectively. (**C**,**D**) Larval eye disc with differentiating ommatidial preclusters posterior to MF, stained with neuronal marker Elav (blue; labeling all photoreceptor nuclei), Bar (red; R1and R6; also indicated in red in A) and Boss (green; labeling R8 in the center of the cluster). (C) Whole disc; (D) a higher magnification of a ventral area. White bars in D indicate the degree of rotation of the respective cluster. Anti-Bar-staining is detected from about a 30° angle to the posterior margin of disc, where all clusters acquire a 90° angle from their original position.

rotation step (45° to 90°) is regulated by *nemo*, a MAP kinase (Choi and Benzer, 1994). A link of *nemo*, Egfr or N-activity to Fz signaling or *rok*-mediated events has not been established. Rotation still takes place in Fz/PCP mutants, albeit at random and mutations in rotation-specific genes do not affect the R3/R4 fate decision and ommatidial chirality. It thus appears likely that distinct signaling inputs are required downstream of Fz/PCP to regulate the mechanistic aspects of ommatidial rotation.

The role of cell-adhesion in ommatidial rotation has not yet been addressed. Cadherins are a conserved family of transmembrane proteins that mediate cell-cell adhesion. They maintain tissue integrity and are required for dynamic processes including cell polarization, cell sorting, tissue segregation, axonal patterning, synaptogenesis and cell migration (Oda et al., 1998; Tepass et al., 2000; Yeaman et al., 1999). Classical cadherins are single pass transmembrane glycoproteins that mediate cell-cell adhesion through their Ca-dependent extracellular domains, which are composed of 'cadherin repeats'. Their cytoplasmic tails interact with the cytoskeleton by binding to catenins, which then recruit other cytoskeletal or signaling proteins (Perez-Moreno et al., 2003). The cadherin-catenin complex, which forms adherens junctions in vertebrates and invertebrates, is dynamically regulated to participate in cell adhesion, sorting and signaling.

Drosophila has three cadherins that are functionally related to vertebrate classical cadherins: DE-cadherin (DE-cad/*shotgun*), expressed in almost all epithelia; and two DN-cadherins (DN-cad1/*cadN* and DN-cad2/*cadN2*), encoded by adjacent genes and predominantly expressed in mesodermal and neural tissues (Iwai et al., 1997; Tepass et al., 1996; Uemura et al., 1996; Prakash et al., 2005). Vertebrate E- and N-cadherins often show complementary expression patterns. Similarly, *Drosophila* DE-cad is early expressed ubiquitously and later is downregulated in newly forming mesoderm and neural tissues, and replaced with DN-cad. This 'cadherin switch' from an epithelial cadherin, maintaining cells in an epithelial layer, to a N-cad that promotes cell migration is a required step during development (Hazan et al., 2004). As cadherins are required to maintain tissue integrity, it is difficult to demonstrate an instructive role in tissue remodeling. However, there is evidence that, in addition to N-cad, E-cad also promotes cell movement (Montero et al., 2005; Niewiadomska et al., 1999).

Studies with Egfr signaling in ommatidial rotation suggest that DE-cad is involved in this process. In particular, decreasing the dose of endogenous DE-cad enhances the rotation specific phenotype of Egfr-signaling components (Brown and Freeman, 2003; Gaengel and Mlodzik, 2003), suggesting that DE-cad is required during rotation. Here, we demonstrate that *shotgun* (*shg/DE-cad*) promotes ommatidial rotation. By contrast, the DN-cadherins appear to restrict rotation, most probably by preventing ommatidia from rotating too fast. Our data indicate that the balance between DE-cad and DN-cad is crucial for the precision required to achieve correct ommatidial rotation. Consistent with this conclusion is the largely complementary subcellular accumulation of DE-cad and DN-cad1 in developing ommatidial preclusters. The dynamic cell-cell adhesion mediated by the two cadherins regulates the extent of motility in several developmental contexts and disease states.

MATERIALS AND METHODS

Fly strains and genetics

UAS-DE-cad transgenes were as described (Lee et al., 2003). For *UAS-DN-cad1*, two independent lines were tested with medium to high expression levels (T. Uemura, personal communication). All were driven with the UAS/Gal-4 system (Brand and Perrimon, 1993). *sevGal4* drives expression in R3/R4, R1/R6 and R7 precursors (gift from K. Basler). The flip-out gain-of-function clones of *UAS-DN-cad* and *UAS-DE-cadDN* were generated with *hs-FLP*, *actin>CD2>Gal4* (Pignoni and Zipursky, 1997) and marked with *UAS-GFP*. Interaction crosses were grown at 25°C and eyes from female flies examined. The transgenes that modified *sev>DE-cadDN* (*UAS-Ecad^{WT}, UAS-EcadEx, UAS-EcadΔB, UAS-Arm^{S2}*) showed no phenotype with *sevGal4* by themselves.

For loss-of-function clonal analyses, *shg^{P34-1}* (gift from U. Tepass) was recombined onto the *w^{-}; FRT42* chromosome and clones were induced with *eyFLP* (marked with *ubiGFP*) (Newsome et al., 2000). Minute (M) clones [giving mutant tissue a growth advantage; Garcia-Bellido et al. (Garcia-Bellido et al., 1976)] were induced with *eyFLP; FRT42, ubiGFP, M*. For rescue experiments, *eyFLP; shg^{P34-1}, FRT42, ubiGFP; sev>DEcad^{WT}* genotype was analyzed.

Mutant alleles and UAS lines: shg^{P34-1}, shg^{R6}, shg^{Ig29} (from U. Tepass), DE-cad^{WT} (UAS-DECH and UAS-DEFL), DE-cadDN (dCR3h 7-1), DE-cad-dEx (UAS-dEx), DE-cadDN (UAS-dCR4h, UAS-dCR4, UAS-dCPc3, UAS-mNcGSP) (see Oda and Tsukita, 1999); UAS-DE-cadΔβ (Pacquelet et al., 2003), ubi-DE-cad-GFP (from F. Schoeck), UAS-DN-cad, Ncad^{M19}

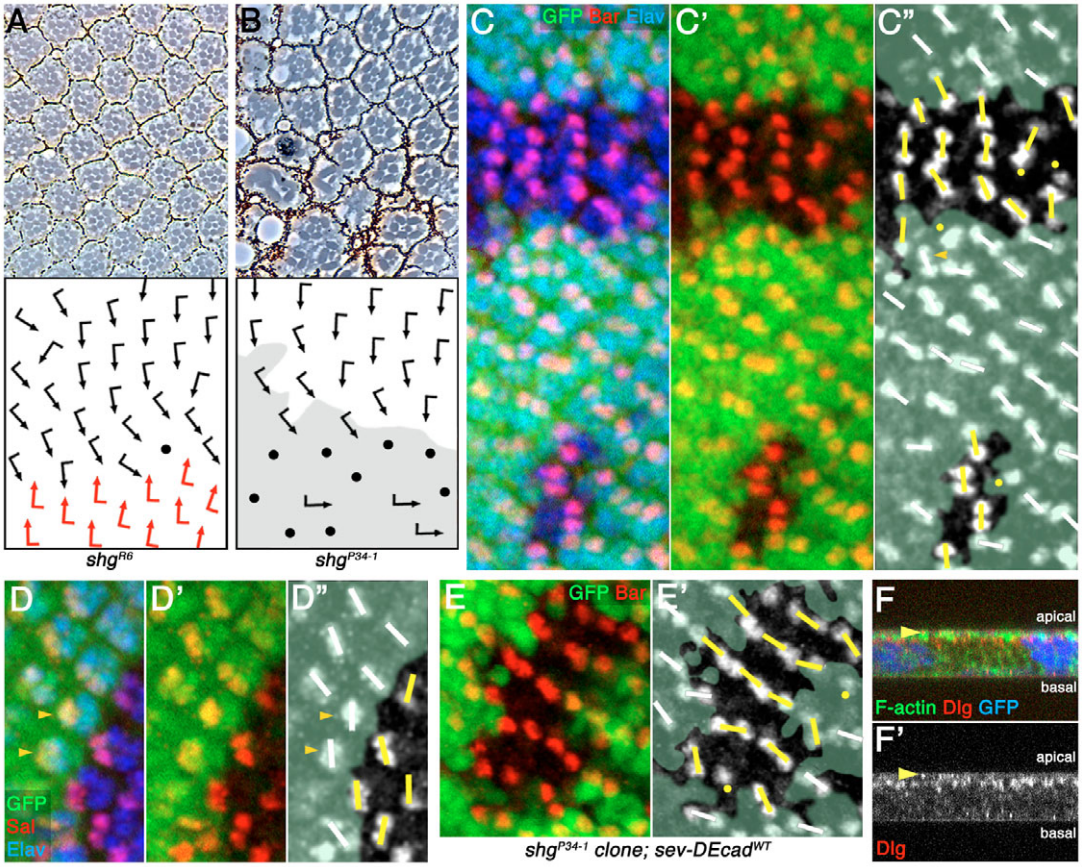

Fig. 2. DE-cadherin promotes rotation. (**A**,**B**) Tangential sections of adult eyes (dorsal is upwards, anterior leftwards) with a schematic representation shown in bottom panels (arrows as in Fig. 1). (A) Eye of homozygous hypomorphic *shg*^{R6} escaper, showing rotation defects with ommatidia often rotating less than 90°. (B) Clone of an intermediate allele, *shg*$^{P34-1}$ (marked by increased pigment levels; grey area in schematic) show rotation defects in addition to severe adhesion defects causing photoreceptor cell loss. (**C-F**) Confocal microscopy images of ventral regions of 3rd instar eye discs (anterior is leftwards, dorsal upwards). (C-C″) Clones of intermediate *shg*$^{P34-1}$ allele. Blue: Elav, all photoreceptors. Red: Bar, labeling R1/R6 and highlighting rotation angle of each cluster. Green: GFP labeling wild-type tissue, mutant clones marked by absence of GFP. Non-rotating ommatidia are present, as visualized by Bar-staining (red in C,C′) in mutant areas. (C″) Semi-schematic version of C′, white bars indicate orientation of wild type and yellow bars indicate orientation of mutant clusters. (D-D″) Clones of *shg*$^{P34-1}$ allele. Rotation is abnormal from its onset: anti-Spalt (Sal in red) is the earliest R3/R4 marker. R3/R4 fate is correctly specified in *shg*$^{P34-1}$ clone, but many ommatidia do not initiate rotation (Elav, blue; GFP, green, marking wild-type tissue). White and yellow bars in D″ are as in C″ (white representing wild-type and yellow mutant clusters). (D′,D″) Orange arrowheads mark preclusters composed of wild-type cells adjacent to mutant tissue that are misrotated, suggesting that *shg/DE-cad* is also required in interommatidial cells for rotation. (E-E′) *sev>DEcad*^{WT} partially rescues rotation in *shg*$^{P34-1}$ clones (Bar, red; GFP, green, marking wild-type tissue). Many mutant preclusters have a 'rescued' rotation angle. (F,F′) Markers of apicobasal polarity are normally localized within *shg*$^{P34-1}$ clones. Discs Large (Dlg; red), apical F-actin (phalloidin, green) and GFP (blue; marking wild-type tissue) are shown. Apical to epithelial disc layer are the squamous cells of the peripodial membrane (yellow arrowhead).

(Iwai et al., 1997), UAS-RhoA^{IR} (Billuart et al., 2001), Ncad$^{\Delta 14}$ (Prakash et al., 2005), UAS-DE-cad^{wt} (Lee et al., 2003), stbm^{6}, and dgo, stbm double mutant (Das et al., 2004). shg^{2}, mys^{1}, UAS-Arm^{S2}, arm^{YD35}, arm^{XM19}, wg^{CX4}, spi^{259}, Egfr^{ElpB1}, pnt^{D88}, fz^{R52}, dsh^{1}, fmi^{E59}, dgo^{380}, nmo^{P}, dRok^{2}, sca^{BP1}, rhoA^{72R} and UAS-GFP are as described in FlyBase (http://flybase.bio.Indiana.edu).

Immunohistochemistry and histology

Primary antibodies used were: rat anti-DE-cad (DCAD2; gift from H. Oda); rabbit anti-Bar (gift from K. Saigo); rat anti-Spalt (from B. Mollereau); rabbit anti-Dlg (gift from Z. H. Chen); mouse anti-γ-tubulin (Sigma), rhodamine-phalloidin (Molecular Probes); anti-β-Gal (Cappel, Promega), rat anti-Elav, mouse anti-Armadillo (N27A1), rat anti-DN-cad (Dn-Ex#8) and mouse anti-Flamingo from Hybridoma Bank. Secondary antibodies coupled to fluorochromes were from Jackson Laboratories. Imaginal discs were stained as described (Fanto et al., 2000), mounted in 80% glycerol/2% N-propyl-gallate and viewed with a Zeiss 510 confocal laser-scanning microscope. Eye sections were prepared as described (Tomlinson et al., 1987). For genetic interactions, eyes were sectioned near equatorial region and only ommatidia with correct photoreceptor number were scored; a rotation defect was defined as being either less than 80° or more than 110° (compared to 90° in wild type).

RESULTS

DE-Cadherin/*shotgun* mutants show defects in ommatidial rotation

To address the role of DE-cad in ommatidial rotation, we first analyzed the eye phenotypes of mutant alleles of *shotgun* (*shg*, the *Drosophila* E-cad gene). A complete loss of DE-cad causes severe cellular defects because of the loss of tissue integrity and, thus, precludes the analysis of ommatidial rotation. However, several hypomorphic *shg* alleles exist that retain enough activity to allow for normal early epithelial development and, thus, the analysis of PCP associated defects. Eye sections from a viable weak hypomorphic allele, *shg*^{R6}, show areas where many ommatidia

have rotated less than 90° (Fig. 2A; stronger alleles do not allow for an analysis in adult eyes, as many photoreceptors are malformed or missing, Fig. 2B). Next, we analyzed somatic eye imaginal disc clones of an intermediate *shg* allele ($shg^{P34\text{-}1}$) using the FRT/FLP method. This allowed us to test whether the effect on rotation is a consequence of DE-cad/*shg* function at the time when ommatidial rotation is taking place, and to analyze the phenotypes of stronger *shg* alleles. Using several markers, including anti-Bar staining, we were able to highlight the rotation angle of the R1/R6 cell pair and, thus, the whole ommatidial cluster (Fig. 1C,D). In late 3rd instar larval discs, when ommatidial rotation occurs, clones of $shg^{P34\text{-}1}$ show robust rotation defects (Fig. 2C-C″). Within mutant tissue, about 50% of ommatidia do not initiate rotation and several others rotate less in comparison with wild-type clusters of the same stage (Fig. 2C-C″,E-E″ and Table 1). Rotation defects are apparent both in small and large mutant clones, where most of the eye is homozygous for $shg^{P34\text{-}1}$ (Fig. 2C-C″ and not shown). Rotation defects are apparent from its initiation as detected with the early R3/R4 marker Spalt (Fig. 2D,D′). We also tested for apicobasal polarity defects with specific markers (see Materials and methods), and found no evidence for significant apicobasal polarity defects (Fig. 2F,F′ and not shown). Specification of R3/R4 cell fates was also largely normal (Fig. 2D).

These data indicate that the rotation phenotype is a primary defect and not due to a general disorganization of the epithelium. Taken together, this indicates that *shg*/*DE-cad* is required to promote ommatidial rotation.

DE-Cadherin is positively required for ommatidial rotation

To further examine the role of DE-cad in rotation, we used the UAS/Gal4 system (Brand and Perrimon, 1993) to analyze the consequences of eye specific expression of different forms of the DE-cad protein (Oda and Tsukita, 1999) (see Materials and methods). In addition to full-length protein, transgenic lines with deletions of either the entire extracellular, intracellular or deletions in cadherin (CAD) repeats were tested (see Materials and methods). Expression of full-length DE-cad under the control of *sevGal4* (expressed in the R3/R4 pair at the time of rotation initiation; see Materials and methods) had no effect at moderate levels, and caused epithelial defects at high levels (not shown). By contrast, a *sevGal4* driven dominant-negative construct [*DE-cadDN*, with an internal deletion of two CAD repeats; (Oda and Tsukita, 1999)] resulted in specific rotation defects (*sev>DE-cadDN*; Fig. 3A). Importantly, as photoreceptor loss and patterning defects were minimal and PCP associated chirality defects were not observed, this suggested that DE-cad specifically affects ommatidial rotation. This phenotype is comparable with *rok* or *nemo* (Choi and Benzer, 1994; Winter et al., 2001), which also specifically affect rotation but not the R3/R4 fate decision. We confirmed that *DE-cadDN* indeed acts as a dominant negative, as removing one copy of endogenous *DE-cad*/*shg* enhanced the *sev>DE-cadDN* phenotype (Fig. 3B). Moreover, co-expression of $DE\text{-}cad^{WT}$ (moderate levels) with *DE-cadDN* (under *sevGal4* control) rescued the rotation defects (Fig. 3C).

A striking feature of all rotation defects associated with the DE-cad loss-of-function phenotypes (either in hypomorphic allele, shg^{R6}, $shg^{P34\text{-}1}$, or *DE-cadDN* combinations) is that the majority of ommatidia rotate less than 90°, displaying variable levels of under-rotation or lacking rotation completely (Fig. 2A-E; Fig. 3A,B; Table 1). The severity of the under-rotation correlates with allelic strength (see Fig. S1 in the supplementary material). The above data indicate that *DE-cad*/*shg* acts as a positive regulator of ommatidial rotation.

Dynamic expression of DE-cad and DN-cad during ommatidial rotation

We next analyzed the expression pattern of DE-cad during ommatidial rotation. E-cad is expressed uniformly in epithelia close to the apical cell surface, establishing adherens-junctions through its homophilic cell-adhesion behavior and its intracellular interactions with the cytosolic catenins (Perez-Moreno et al., 2003). Similarly, in the eye disc epithelium, prior to photoreceptor recruitment and adjacent to the furrow (MF), DE-cad is equally distributed as an apicolateral membrane 'ring' in all cells (Fig. 4A-A′, left of MF). Posterior to MF, DE-cad expression is patterned (Fig. 4A,A′, right of MF). As photoreceptor precursors are recruited into preclusters, DE-cad becomes enriched in membranes bordering R8, and the R2/R5 pair (Fig. 4A,A′, see Fig. 4D,D″ for detail), and interestingly it is detected at much lower levels at the membranes between the R3/R4 pair, as well as membranes between precluster cells and surrounding undifferentiated cells (Fig. 4A,A′,4D,D″). DE-cad remained upregulated at all membranes between precluster cells, except the R3/R4 border, throughout the process of rotation and precluster assembly (Fig. 4A).

The *Drosophila* β-catenin protein Armadillo (Arm) colocalizes with DE-cad through its interaction with cytoplasmic DE-cad sequences (Tepass et al., 2000). Interestingly, Arm is still enriched at the R3/R4 border where DE-cad expression is low (Fig. 4A, arrows; Fig. 4D,D′), suggesting that Arm interacts with another cadherin. We, thus, analyzed DN-cad1 expression and observed that its distribution within the precluster is largely complementary to DE-cad; DN-cad1 is enriched at R3/R4 cell border membranes (Fig. 4B,C,4E-E″). DN-cad1 is not detected ahead of and close to the MF (Fig. 4C). Later, DN-cad1 is also detected in axonal projections of all photoreceptors as these extend out of the retinal layer (Lee et al., 2001; Prakash et al., 2005). At the apical R3/R4 border, DN-cad1 colocalizes with the atypical cadherin Flamingo [Fmi; a core PCP-signaling and R3/R4 specification factor (Das et al., 2002)] (Fig. 4E).

To gain insight as to how the DE-cad and DN-cad1 complementary accumulations are generated within the precluster, we analyzed their localization in loss-of-function and overexpression clones of each other (see Materials and methods).

Table 1. Rotation angle distributions in *shg/DE-cad* and *DN-cad* mutant clones

Genotype	*n*	0-10°	10-30°	30-60°	60-80°	80-100°	>100°
Wild type	198		2%	88%	8%	2%	
$shg^{P34\text{-}1}$	256	51%	20%	17%	12%	1%	
$shg^{P34\text{-}1}$; $sev>DE\text{-}cad^{WT}$	157	20%	20%	29%	27%	4%	
$Ncad^{\Delta 14}$	165		1%	28%	31%	36%	4%

The angles were scored in the first seven columns that stain with anti-Bar. In this region in wild type, most clusters (88%) are rotated ~45±10° (30-60°). In the loss-of-function $shg^{P34\text{-}1}$ mutant, the majority of clusters have not rotated at all (51%) or are severely under-rotated (20%). By contrast, in $Ncad^{\Delta 14}$ (a small deficiency removing both genes, *cadN1* and *cadN2*), many clusters have reached the 90° angle prematurely or have even over-rotated. The $shg^{P34\text{-}1}$; $sev>DE\text{-}cad^{WT}$ genotype causes a partial rescue of the $shg^{P34\text{-}1}$ loss-of-function mutant phenotype, but also leads to a spreading of rotation angles, suggesting deregulated DE-cad activity. Data are collected from larval eyes.

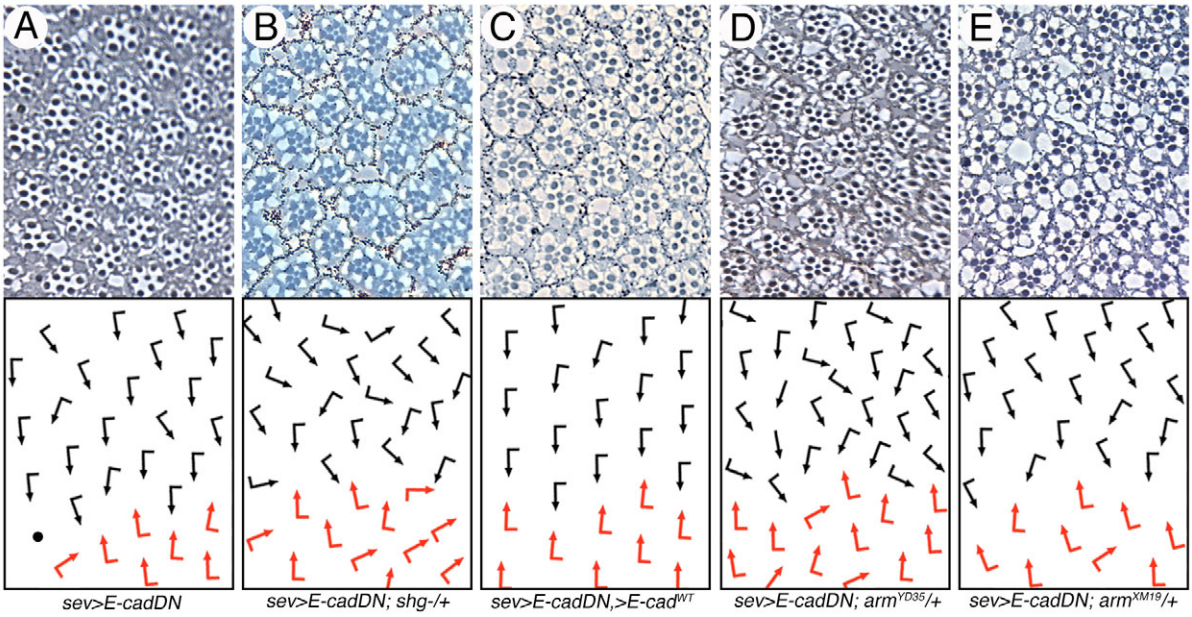

Fig. 3. DE-cad requirements for ommatidial rotation. Tangential sections of adult eyes are shown (dorsal is upwards, anterior leftwards); associated bottom panels show schematic representations (arrows as in Fig. 1). (**A**) *sevGal4; UAS-DE-cadDN* (*sev>DE-cadDN*), a dominant-negative construct with two internally deleted CAD repeats, causes under-rotation. The under-rotation is enhanced by decreasing endogenous *DE-cad/shg* (**B**; *sev>DEcadDN; shg*$^{-}$/+), and is suppressed by co-expression of full-length DE-cad (**C**; *sev>DEcadDN;sev>DE-cad*^{WT}). (**D**) Decreasing endogenous Arm (*arm*^{YD35}/+, null allele) enhances under-rotation and adhesion defects of *sev>DE-cadDN*. (**E**) *arm*^{XM19}, an *arm* allele defective for Wg signaling, but functional for cell adhesion, does not modify the *sev>DE-cadDN* phenotype.

First, we determined the contribution of DE-cad and DN-cad1 to apicolateral Arm localization. DE-cad levels strongly affect Arm levels (Fig. 4G), suggesting that the bulk of endogenous apicolaterally localized Arm is anchored through DE-cad, the exception being the R3/R4 cell border membranes. By contrast, decrease in DN-cad1 and 2 levels (Fig. 4F) has no effect on DE-cad (not shown) or Arm, except at the R3/R4 border, where Arm levels are reduced (Fig. 4F,F′). The DN-cad1 expression pattern is unchanged in *DE-cad/shg* (*shg*$^{P34\text{-}1}$) loss-of-function clones (Fig. 4G,H). Arm is significantly decreased in such clones, but still accumulates apicolaterally between the precluster cells, where DN-cad is present (Fig. 4G). Clones overexpressing DE-cadDN do not affect endogenous DN-cad1 or Fmi (not shown). However, an increase in DN-cad1 expression lowers DE-cad levels (Fig. 4I,I′), without affecting Fmi localization (Fig. 4I,I″; the same is observed anterior to MF, not shown). Both DN-cad1 and DE-cadDN overexpression causes an increase in membrane associated Arm (Fig. 5E; not shown). These data indicate that there is largely mutually exclusive localization of DE-cad and DN-cad1 in wild type. The regulation of this pattern might be in part mediated through a repressive effect of DN-cad on DE-cad, as observed in the gain-of-function DN-cad clones (Fig. 4I). However, it is more complex, as in *DN-cad* mutant clones DE-cad is not upregulated.

DN-cadherins are required to restrict rotation

The complementary accumulation of DE- and DN-cad1 within the precluster and the concentration of DN-cad1 at the R3/R4 border prompted us to examine a potential role for DN-cad in rotation. As noted previously, *Drosophila* has two DN-cadherin genes (Prakash et al., 2005). Although single loss-of-function analysis did not show a retinal phenotype, mosaic eyes of mutants lacking both genes [*DN-cad*$^{\Delta 14}$ deletes *DN-cad1* and *DN-cad2* (Prakash et al., 2005)] revealed retinal phenotypes, including misrotated ommatidia, symmetrical clusters and loss of photoreceptor cells (Fig. 5A, and not shown)**.**

To gain better insight into the role of DN-cad in rotation, we analyzed *N-cad*$^{\Delta 14}$ clones in 3rd instar eye discs, during ommatidal rotation and prior to terminal photoreceptor differentiation [also affected in the *N-cad*$^{\Delta 14}$ mutant (Prakash et al., 2005)]. Interestingly, the disc phenotype of *N-cad*$^{\Delta 14}$ mutant clusters is the opposite of *DE-cad/shg* mutant clones, with the majority of mutant ommatidial clusters reaching a 90° angle prematurely as compared with wild-type neighbors (Fig. 5B; Table 1). Therefore, DN-cad function appears to provide the correct rate of movement.

We next tested the effects of DN-cad1 overexpression, driven with *sevGal4* (*sev>DN-cad*). The *sev>DN-cad* genotype showed rotation defects reflected in ommatidia having rotated to a random degree (Fig. 5F). Random rotation angles are also observed in 3rd instar *sev>DN-cad* eye discs (Fig. 5C), consistent with the loss-of-function analysis and the suggestion that the DN-cadherins function in controlling the rate of rotation.

DE-cad affects rotation through its interactions with cytoskeletal elements

To gain further insight into cadherin requirements in ommatidial rotation, we used the dose-sensitive *sev>DE-cadDN* and *sev>DN-cad* genotypes for dominant genetic interaction studies. This approach is often used in *Drosophila* to identify members of a signaling pathway or interacting factors involved in the regulation of a particular developmental or morphological process (e.g. Boutros et al., 1998; St Johnston, 2002). Our initial analysis of *sev>DE-cadDN* indicated that the phenotype is dose sensitive and modified by decreasing endogenous DE-cad levels (Fig. 3B).

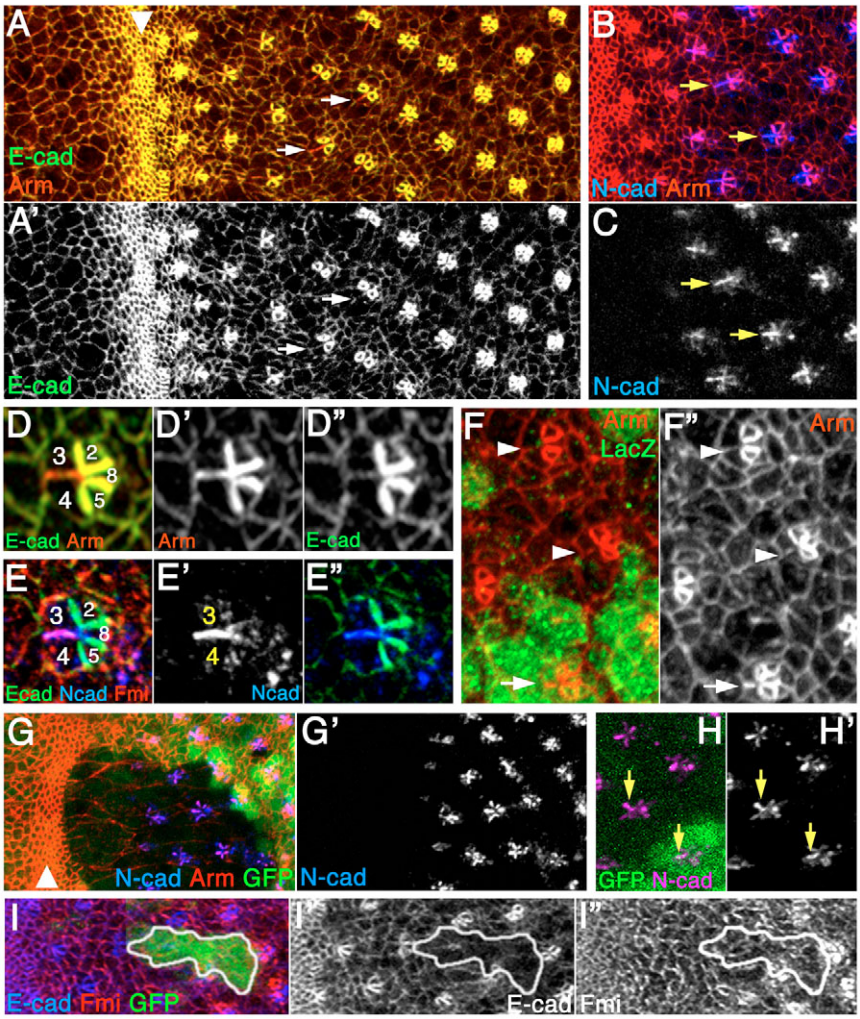

Fig. 4. Complementary distribution of DE- and DN-cadherins during ommatidial rotation. All panels show confocal microscopy images of 3rd instar eye discs (anterior is leftwards, dorsal is upwards). (**A**) DE-cad (green) and Arm (red). Enriched staining is found in morphogenetic furrow (MF, white arrowhead) and within precluster cells (see also D and E for high-magnification images). Arm and DE-cad overlap, except at R3/R4 border, where DE-cad is almost absent (examples indicated by arrows). (**B**) Arm (red), DN-cad1 (blue). (**C**) Enriched DN-cad staining is present at the R3/R4 cell border (arrows in B,C; see also E for high magnification.) (**D**,**E**) High magnification of preclusters stained for DE-cad (green) and Arm (red) in D-D″, and DE-cadGFP (green), DN-cad (blue) and Fmi (red) in E-E″. DE-cad and DN-cad1 distribution is largely non-overlapping (E″). (**F-I**) DE-cad and Arm localization analyses in mutant backgrounds. (F) Arm (red) localization in *N-cad*$^{\Delta 14}$ clones (marked by absence of LacZ). Arm is reduced only at the R3/R4 border membrane (examples marked by arrowheads; compare with wild type marked by arrow). (G) Arm (red) and DN-cad (blue and G′) in *shg*$^{P34\text{-}1}$ mutant tissue. Arm is almost completely lost from apicolateral membranes, except where it co-localizes with DN-cad (which is not affected). (H). Example of DN-cad1 distribution in *shg*$^{P34\text{-}1}$ clone (wild type marked by GFP: green): accumulation at R3/R4 border is unchanged (see arrowheads). (I-I″) Overexpression of DN-cad1 (marked by GFP; green) reduces DE-cad (blue and I′), but not Fmi (red and I″) levels.

We first tested mechanistic aspects of DE-cad-regulated rotation. The *sev>DE-cadDN* phenotype is enhanced by dose reduction of an *arm* null allele (*arm*^{YD35}; Fig. 3D), but not an *arm* allele that maintains its cell architecture function (*arm*^{XM19}, only defective for Wg-signaling; Fig. 3E). This suggests that the cytoskeletal anchoring function of DE-cad, via Arm/β-catenin, is crucial for ommatidial rotation, and is supported by several observations. First, the enhancement is, in addition to rotation, in defects associated with ommatidial architecture and adhesion (Fig. 3D; e.g. causing gaps between ommatidia; also Fig. 5G). Second, unlike full-length DE-cad that rescues the rotation defects of *sev>DE-cadDN* (Fig. 3C), co-expression of *sev>DE-cadDN* with *DE-cadΔβ*, which lacks Arm interaction sequences, does not rescue the defects (Table 2). Third, DE-cad lacking the extracellular Cad-repeats (*DE-caddEx*) does not rescue *sev>DE-cadDN* when co-expressed (Table 2). Taken together, these data suggest that the cell adhesion and cytoskeletal anchoring aspects of DE-cad are crucial in ommatidial rotation.

To further define the relationship of DE-cad and DN-cad in rotation, we tested their genetic interactions. Whereas *sev>DE-cadDN* associated under-rotation is enhanced by co-expression of DN-cad, it is not affected by dose reduction of DN-cad loss-of-function alleles (*N-cad*$^{\Delta 14}$; Table 2). The *sev>DN-cad* phenotype is enhanced both by *DE-cad/shg* dose reduction and by co-expression of DE-cad^{WT} (not shown). The enhancement of *sev>DE-cadDN* under-rotation by co-expression of DN-cad may be due to competition for Arm (as suggested from DN-cad gain-of-function clones; Fig. 5E,E′). However, the *sev>DN-cad* rotation phenotype is not enhanced by *arm* reduction (Fig. 5G) and co-expression of *UAS-Arm*^{S2} (full-length) enhances both the rotation defects and defects in epithelial integrity of *sev>DN-cad* (Fig. 5H). Taken together, these observations suggest that a proper balance between DE-cad, DN-cads, and Arm levels is crucial for the precise 90° ommatidial rotation.

PCP and Egfr-signaling components interact with the DE-cad rotation phenotype

The direction of rotation is regulated by Fz/PCP signaling (Adler, 2002; Klein and Mlodzik, 2005; Mlodzik, 1999; Strutt and Strutt, 1999). Egfr-signaling is also required for the process, although its specific regulatory input remains unclear (Brown and Freeman, 2003; Gaengel and Mlodzik, 2003; Strutt and Strutt, 2003). We thus tested for genetic interactions of components of these pathways with *sev>DE-cadDN*.

Previous studies identified *shg*/*DE-cad* alleles as enhancers of rotation defects caused by reduction in Egfr signaling (Brown and Freeman, 2003; Gaengel and Mlodzik, 2003) (a decrease in DE-cad enhances the randomness of rotation in Egfr-signaling mutants). Our data show that reduced Egfr-signaling levels (e.g. reduced gene dose of the Egfr-ligand Spitz) specifically enhanced the under-rotation of *sev>DE-cadDN* (Table 2), suggesting that Egfr-signaling promotes

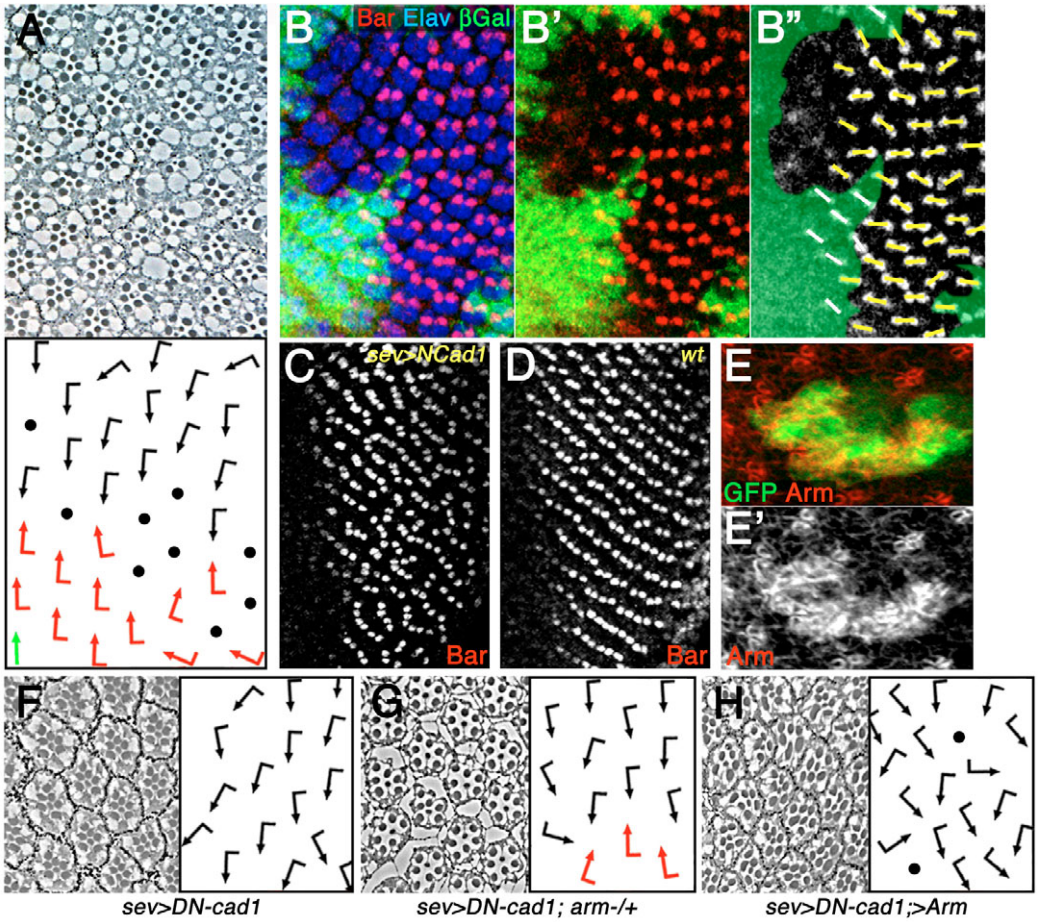

Fig. 5. *DN-cad1* and *DN-cad2* are required for normal ommatidial rotation. (**A**,**B**) *N-cad*$^{\Delta 14}$ double mutant clones in adult eyes (A) and eye discs (B-B″). (A) A mosaic eye containing *N-cad*$^{\Delta 14}$ clones (owing to the nature of the allele, the clone cannot be marked). Several clusters with rotation defects are present (dots in schematic indicate ommatidia with photoreceptor loss that cannot be scored for rotation). (B-B″) Ventral part of eye disc with *N-cad*$^{\Delta 14}$ clone marked by absence of βGal (green), stained for Elav (blue) and Bar (red); in semi-schematic (B″), the rotation angles are indicated with white (wild-type clusters) or yellow (mutant or mosaic clusters) bars. Most mutant clusters are over-rotated relative to their stage. (**C**) *sev>DN-cad1* eye disc, Bar staining highlights random rotation throughout the disc (**D**, Bar-staining in wild-type disc for comparison). (**E**) Clone of cells overexpressing DN-cad1 (GFP). Localization of Arm (red and E′) to plasma membranes and cytoplasmic membrane compartments is increased in the clone. (**F-H**) *sev>DN-cad1* is suppressed by gene dose reduction in *arm* (*sev>DN-cad1/arm*^{4}; compare G with F). Gaps between ommatidia resulting from decreased adhesion (although rotation defects are not enhanced by Arm decrease) and enhanced by Arm co-overexpression (*sev>DN-cad1;>Arm*^{S2}; H).

rotation by positively regulating DE-cad function. This is supported by the observation that the gain-of-function *Egfr*^{Elp} allele appears to suppress *sev>DE-cadDN* under-rotation (not shown; owing to the dominant effects of *Egfr*^{Elp} on photoreceptor numbers and survival this effect cannot be directly compared with the other interactions). The enhancement of *sev>DE-cadDN* by *pointed* (Table 2; *pnt*, a common nuclear effector of RTK/MAPK pathways) suggests that the entire RTK/MAPK cascade is functioning in this context (see Discussion).

The complementary DE- and DN-cadherin accumulation within the R3/R4 pair, which is crucial for PCP establishment (see Introduction), suggested a possible link between PCP components and cadherin function. Although reduction in Fz and Dsh, the upstream components of Fz/PCP-signaling did not modify *sev>DE-cadDN*, mutations in the PCP genes *stbm* and *dgo* enhanced *sev>DE-cadDN*, as did reduction of RhoA, an effector of Fz/PCP-signaling downstream of Dsh (Table 2; Fig. 6A,B).

We next wished to determine whether *DE-cad/shg* during rotation is required in a specific cell or cells within the precluster, and in particular tested for R3/R4 requirement. Mosaic analysis of *shg*$^{P34-1}$ clones (in discs) suggested that mosaic ommatidia with both R3 and R4 wild type do not have a higher probability of rotating normally. Largely, the overall number of wild type R-cells correlates with correct rotation: the more wild-type cells are present per cluster, the higher is the probability of normal rotation (see Tables and Fig. S1 in the supplementary material). Furthermore, we have also observed fully wild-type preclusters directly adjacent to mutant interommatidial cells that failed to rotate properly (Fig. 2C-D″; orange arrowheads), suggesting that *DE-cad/shg* function is required not only in R-cells but also in adjacent interommatidial cells. Nevertheless, expression of *sev>DEcad*^{WT} (expressed in R3/R4 at the onset of rotation) increased the number of clusters that initiated rotation in *shg*$^{P34-1}$ clones (Fig. 2E,E′; Table 1), suggesting that sufficient levels of DE-cad in R3/R4 are crucial. Taken together,

Table 2. *sev>E-cadDN* rotation phenotype is dominantly enhanced or suppressed by components of adherens junctions, and by EGFR and PCP signaling pathways

	*sev>EcadDN/**	Under-rotated ommatidia (%)	Effects*	*n*
Cell adhesion	w^{1118} *(wild type)*	10.7±1.5	Control	500
	shg^{lg29}	35.8±10.2	Enhancer	404
	shg^{2}	42.9±13.4	Enhancer	340
	$shg^{P34\text{-}1}$	27.9±7.8	Enhancer	561
	UAS-Ecad^{WT}	1±1	Suppressor	386
	UAS-EcaddEx	6.7±1.5	None	464
	UAS-Ecad$\Delta\beta$	10.7±0.6	None	504
	$Ncad^{M19}$	9.5±3	None	404
	$Ncad^{\Delta 14}$	12±3	None	437
	UAS-DNcad^{wt}	39±2.6	Enhancer	450
	mys^{1}	7.3±2.1	None	424
PCP/EGFR/rotation	spi^{259}	25±7 4	Enhancer	428
	$pnt^{\Delta 88}$	28±11.5	Enhancer	412
	fz^{R52}	11±5.2	None	485
	dsh^{1}	6.7±1.1	None	490
	fmi^{E59}	8.3±5.9	None	465
	dgo^{380}	19.7±2.1	Enhancer	434
	$stbm^{6}$	33±7 3	Enhancer	468
	dgo^{380},$stbm^{6}$	42.6±6	Enhancer	331
	nmo^{P}	14±1.7	None	386
	sca^{BP1}	11±6	None	382
	$dRok^{2}$	11.7±7.5	None	495
	$rhoA^{72R}$	20±8.7	Enhancer	437
	UAS-RhoA^{IR}	27.3±4.7	Enhancer	389
	UAS-GFP	7.7±1.5	Control†	462

*The effects highlighted as enhancers or a suppressor are statistically significant (P<0.01; t-test). Data are collected from adult eyes.
†The *UAS-GFP* served as a wild-type control background for genotypes with co-expression under *sev-Gal4* control.

these data suggest that in rotation *DE-cad/shg* is required in more cells than the R3/R4 pair, including cells that are adjacent but outside the precluster. Moreover, the genetic interactions suggest that parallel input from PCP and Egfr-signaling regulates DE-cad activity during rotation.

RhoA might link PCP signaling to DE-cad function in rotation

Classical cadherins have multiple links to the cytoskeleton, primarily through α- and β-catenin (Perez-Moreno et al., 2003). Reduction of the Fz/PCP effector RhoA enhanced the *sev>DEcadDN* phenotype. Mutants in *rok*, a downstream effector of RhoA, have a rotation-specific loss-of-function eye phenotype, and RhoA has been linked to the regulation of DE-cadherin apical localization and clustering at the membrane (Bloor and Kiehart, 2002; Magie et al., 2002; Yap and Kovacs, 2003).

Our genetic interactions have revealed that decreasing endogenous RhoA levels enhanced the rotation and adhesion defects of *sev>DEcadDN* (Table 2; and not shown). To minimize the RhoA-associated defects that are not linked to rotation [e.g. general cellular architecture as *RhoA* null clones are cell lethal (Strutt et al., 1997)], we expressed *UAS-RhoA*^{IR} [lowering endogenous *RhoA* levels through RNA interference (Billuart et al., 2001)] in the R3/R4 precursors. Co-expression of *sev>DEcadDN* with *UAS-RhoA*^{IR} causes a specific enhancement of the *sev>DE-cadDN* under-rotation phenotype (Fig. 6A,B; Table 2). Whereas a general decrease in endogenous RhoA affects cell adhesion (in addition to rotation), the specific RhoA RNAi knock-down in a subset of R-cell precursors at the onset of rotation only enhances ommatidial under-rotation (Table 2; and not shown). Clones of hypomorphic *RhoA* alleles display an irregular DE-cad localization in eye discs, with malformed preclusters and a general reduction of DE-cad levels outside the precluster (Fig. 6C,C′) (see also Bloor and Kiehart, 2002; Magie et al., 2002; Yap and Kovacs, 2003). Similar results were obtained with $dRok^{2}$ clones (not shown). These data show that in addition to the proposed role for RhoA in DE-cad localization and maintenance of tissue integrity, the dynamic rearrangements of DE-cad and DN-cad during rotation require RhoA function. Fz/PCP-signaling thus probably regulates DE-cad function and/or localization through RhoA-Rok. The fact that we do not observe gross mislocalization of DE-cad in mutant clones of primary PCP genes (e.g. *fmi* or *stbm*; not shown) suggests that effects of RhoA on DE-cad localization/activity in rotation are subtle, influenced by several inputs and not affecting tissue integrity.

DISCUSSION

Here, we have demonstrated that a balance of the classical cadherins DE-cad and DN-cad regulate ommatidial rotation during *Drosophila* eye development. DE-cad promotes the movement of photoreceptor preclusters relative to the surrounding epithelial cells and DN-cadherins act to restrict the rate of movement. Furthermore, the data indicate that DE-cad is affected by PCP and Egfr signaling, thus integrating input from several pathways. A similar requirement for DE-cad in cell movement is also observed in border cell migration during *Drosophila* oogenesis (Niewiadomska et al., 1999). We propose that such conserved molecular mechanisms drive cell movement processes in general during development and disease (see below).

DE-cadherin and cell movement

Although the role for DE-cad in tissues undergoing rearrangements during development is established (Tepass et al., 2000; Perez-Moreno et al., 2003), a direct role for DE-cad in cell and tissue movement has been more difficult to study in vivo owing to its essential role in maintenance of epithelial integrity. Analysis of adult eye phenotypes of a homozygous viable *shg/DE-cad* allele and a

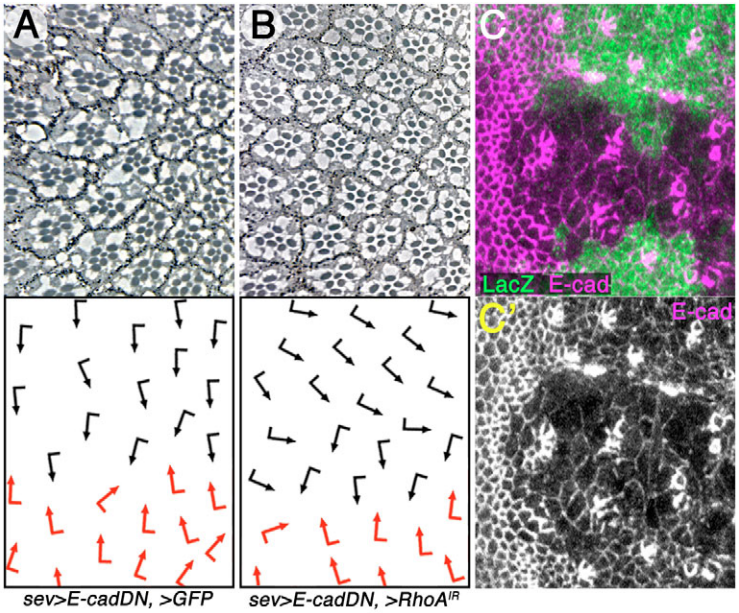

Fig. 6. RhoA affects DE-cad function in rotation and localization. (**A**,**B**) Tangential sections of adult eyes of the following genotypes (anterior is leftwards and dorsal upwards). (A) Co-expression of *sev>DEcadDN* with *UAS-GFP* (control). (B) Co-expression of *sev>DEcadDN* with *UAS-RhoA^{IR}*. *UAS-RhoA^{IR}* enhances under-rotation associated with *sev>DEcadDN* (compare A with B). Arrows are as in Fig. 1. (**C**) Confocal microscopy image of DE-cad (magenta and C′) localization in rhoA^{72R} clones (hypomorphic allele). DE-cad distribution within nascent ommatidial preclusters is disorganized, the overall DE-cad levels are reduced posterior to MF. Green: GFP labeling wild-type tissue.

dominant-negative DE-cad construct (*DE-cadDN*), expressed in the R3/R4 and later R1/R6, R7 precursors, indicate that DE-cad is required throughout the rotation process. The ability of ommatidia to complete the precise 90° rotation directly depends on DE-cad activity. Both the extracellular domain, responsible for cell-cell adhesion, and the intracellular domain, linking DE-cad to the actin cytoskeleton, are required for rotation. DE-cad associates with the actin cytoskeleton primarily through interactions with Arm/β-catenin. Although β-catenin has a dual role in cell adhesion and Wg signaling [which can be separated (Orsulic and Peifer, 1996; Sanson et al., 1996)], our data indicate that during ommatidial rotation β-catenin acts through its role in cell adhesion.

Ommatidial rotation represents the final step in establishing PCP during eye development. The direction of rotation depends on proper R3/R4 cell fate specification, which is determined by PCP signaling. The Egfr pathway and input by rotation-specific genes, e.g. *nemo*, are thought to function in parallel to Fz-PCP signaling. We observed an enhancement of the *sev>DE-cadDN* rotation defects by dose reduction in core regulatory PCP genes *dgo* and *stbm* (Table 2; see Fig. S1 in the supplementary material; ommatidial under-rotation and the number of ommatidia that did not initiate rotation in *sev>DE-cadDN/dgo$^{-/+}$*, *stbm$^{-/+}$* was comparable with the enhancement of *sev>DE-cadDN* by heterozygosity of a *shg* null allele). The localization of PCP protein complexes at the level of adherens junctions (Djiane et al., 2005; Wu et al., 2004) is consistent with the idea that PCP factors can influence DE-cad function. The mechanism of this regulation remains unclear. The *RhoA-RNAi* transgene, which was expressed only in R3/R4 precursors during the initiation of ommatidial rotation, enhanced *sev>DE-cadDN* associated under-rotation defects. Although a RhoA requirement in multiple cellular processes makes it difficult to dissect its specific role in rotation, the specificity of the phenotype (enhanced under-rotation in *sev>DEcad/RhoA^{IR}*) suggests a role for RhoA in the regulation of cadherin-mediated cell movement.

Although Egfr signaling appears to be required for the precise 90° rotation (Brown and Freeman, 2003; Gaengel and Mlodzik, 2003; Strutt and Strutt, 2003), its role in the process – promoting motility or antagonizing it – has remained unclear. Our genetic data suggest that Egfr signaling acts positively to promote rotation, as a reduction in Egfr signaling enhances the *sev>DE-cadDN* under-rotation phenotype (Table 2, Fig. 7). This may reflect a positive role for Egfr signaling in the regulation of DE-cad activity or turnover at the membrane, as suggested from human tumor cell lines (Lu et al., 2003). Affecting the function of endocytic pathway components can also have an effect on ommatidial rotation (Weber et al., 2003). This might be mediated by Egfr signaling, as is thought to be the case in human cancer cells, leading to recycling and redistribution of E-cad at the plasma membrane (Naora and Montell, 2005).

It is likely that, besides PCP and Egfr signaling, additional pathways act in parallel and/or redundantly to regulate this cell motility aspect. A number of genes essential for rotation, including *nemo* and *scabrous*, have not yet been placed within a particular signaling pathway, suggesting that rotation results from spatiotemporal integration of multiple signaling events, emanating either from within the precluster or from the dynamic cell context within the moving furrow.

Distinct requirements for DN-cad and DE-cad in regulating the rotation process

Drosophila DN-cadherins, which are encoded by the adjacent *cadN* and *cadN2* genes, are the main cadherins expressed in the nervous system. In developing photoreceptors they participate in axon guidance, and in pupal eye discs they mediate terminal patterning of the retina [through specific expression in cone cells (Hayashi and Carthew, 2004; Iwai et al., 1997; Lee et al., 2001; Prakash et al., 2005)]. During PCP establishment, DN-cad1 is concentrated at the border between R3/R4 precursors, in a pattern largely complementary to DE-cad (Fig. 4B,C,E). This suggested a possible combinatorial role for DE-cad and DN-cad in rotation, with DN-cad either providing a structural role in rotating clusters, or participating in signaling cascades that regulate cell movement. Analysis of *DN-cad* mutant clones in discs during rotation demonstrated a specific function, as many mutant clusters have completed rotation well before wild-type clusters of the same stage (Fig. 5B-B″). These data indicate that DN-cadherins function to slow down rotation, serving an opposing function to DE-cad.

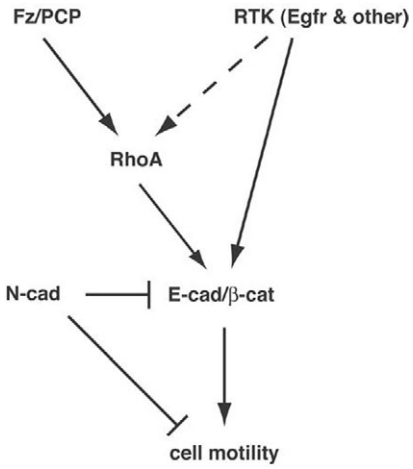

Fig. 7. Model for signaling input into cadherin function in cell motility. DE-cadherin appears to receive positive input from PCP and RTK (e.g. Egfr) signaling, which it translates into directed cell movement. The Egfr input could be either direct (as suggested from cell biology literature) or via nuclear signaling input, as suggested by the observed interaction with the ETS-factor Pointed. DN-cadherin serves as a 'brake' to this movement, and might directly affect DE-cadherin expression. See text for details.

The balance and complementary distribution of DE-cad and DN-cad appear crucial for correct rotation to occur. Mild overexpression of DN-cad1 in R3/R4 (*sev>DN-cad*) is sufficient to interfere with the process, possibly by affecting DE-cad levels. Consistently, DN-cad1 overexpression enhances *sev>DE-cadDN* induced under-rotation and overexpression clones of DN-cad1 cause a decrease in endogenous DE-cad levels (Fig. 4I). Alternatively, the negative effect of DN-cad on DE-cad might be through competition for β-catenin, as *sev>DE-cadDN* is partially rescued by *UAS-Arm*^{S2} (full length; not shown), although as *sev>DN-cad* is not enhanced by *arm* dose reduction this appears less likely. Interestingly, *sev>DN-cad* is enhanced by co-expression of full-length DE-cad and full-length Arm. These phenotypes resemble those of a strong *sev>DN-cad* line (not shown), suggesting that DN-cad is stabilized by increased levels of available Arm, and also that co-overexpression of two cadherins may interfere with optimal turnover rate at the membrane.

In *Drosophila* 'clone 8' (derived from wing discs) cell culture experiments, increased levels of DE-cad cause an increase in Arm levels without changing its mRNA levels (Yanagawa et al., 1997). This is consistent with our data, as overexpression of DN-cad induces apparent accumulation of endogenous Arm in the cell, largely at the cell membrane.

Parallels between ommatidial rotation and cell migration during development and disease

Previous work has identified some signaling input into ommatidial rotation, e.g. PCP and Egfr signaling. Here, we begin to address mechanistic aspects of rotation, defining the involvement of cell adhesion molecules that are linked to cytoskeletal elements.

Ommatidial rotation shares similarities with border cell migration (BCM) during *Drosophila* oogenesis (Niewiadomska et al., 1999). In both cases, DE-cad is upregulated in the cell cluster as the respective cells are being recruited from surrounding epithelial cells, and as migration is initiated, DE-cad is downregulated at the membrane between the migrating cells and surrounding 'substrate' cells. Egfr signaling is required positively for both processes (Duchek and Rorth, 2001) (this work). Thus, although the regulatory role for Egfr in rotation is complex, our data suggest that both Egfr and PCP components promote DE-cadherin mediated rotation. Other RTKs may act redundantly in promoting rotation (I.M. and M.M., unpublished), as they do in BCM (Duchek et al., 2001). Although the role of DN-cad in BCM remains unclear, existing data suggest that it may serve an inhibitory function there. DN-cad1 is detected in all epithelial follicular cells from which border cells are recruited but is lost after mid-oogenesis when BCM initiates (Tanentzapf et al., 2000). Our data suggest that DN-cad1 is initially present, albeit reduced, in border cells, but becomes undetectable during BCM (I.M. and M.M., unpublished).

A positive role for DE-cad in migration is not limited to *Drosophila*. A recent study addressing zebrafish gastrulation finds a similar role for E-cad during cell migration (Montero et al., 2005). Furthermore, BCM (Naora and Montell, 2005) and ommatidial rotation (this work) share similarities with the progression of ovarian carcinoma (Naora and Montell, 2005). Ovarian cancer cells tend to cluster and metastasize as cell aggregates that show upregulation in E-cad expression. The proposed role for RTK signaling in the three processes (BCM, ommatidial rotation and ovarian carcinoma metastasis) suggests an evolutionarily conserved mechanism that can switch the function of E- and N-cad between promoting and inhibiting cell movement.

We are grateful to H. Oda, U. Tepass, T. Uemura, P. Rorth, T. Clandinin, Z. Chen, K. Saigo, K. Basler, L. Luo, F. Schoeck and the Bloomington stock center for flies and reagents; and to K. Gaengel for help with Fig. 1. We thank G. Das, D. Del Alamo, J. Delaney, T. Klein, J. Reynolds-Kenneally and U. Weber for comments on the manuscript; members of the Mlodzik laboratory for useful discussions; and C. Tan and M. Burnett for technical help. This work was supported by NIH/NEI grant RO1 EY14597 to M.M.

Supplementary material

Supplementary material for this article is available at http://dev.biologists.org/cgi/content/full/133/17/3283/DC1

References

Adler, P. N. (2002). Planar signaling and morphogenesis in Drosophila. *Dev. Cell* **2**, 525-535.

Bellaiche, Y., Gho, M., Kaltschmidt, J. A., Brand, A. H. and Schweisguth, F. (2001). Frizzled regulates localization of cell-fate determinants and mitotic spindle rotation during asymmetric cell division. *Nat. Cell Biol.* **3**, 50-57.

Billuart, P., Winter, C. G., Maresh, A., Zhao, X. and Luo, L. (2001). Regulating axon branch stability: the role of p190 RhoGAP in repressing a retraction signaling pathway. *Cell* **107**, 195-207.

Bloor, J. W. and Kiehart, D. P. (2002). Drosophila RhoA regulates the cytoskeleton and cell-cell adhesion in the developing epidermis. *Development* **129**, 3173-3183.

Boutros, M., Paricio, N., Strutt, D. I. and Mlodzik, M. (1998). Dishevelled activates JNK and discriminates between JNK pathways in planar polarity and *wingless* signaling. *Cell* **94**, 109-118.

Brand, A. H. and Perrimon, N. (1993). Targeted gene expression as a means of altering cell fates and generating dominant phenotypes. *Development* **118**, 401-415.

Brown, K. E. and Freeman, M. (2003). Egfr signalling defines a protective function for ommatidial orientation in the Drosophila eye. *Development* **130**, 5401-5412.

Choi, K.-W. and Benzer, S. (1994). Rotation of photoreceptor clusters in the developing *Drosophila* eye requires the *nemo* gene. *Cell* **78**, 125-136.

Chou, Y. H. and Chien, C. T. (2002). Scabrous controls ommatidial rotation in the Drosophila compound eye. *Dev. Cell* **3**, 839-850.

Cooper, M. T. D. and Bray, S. J. (1999). Frizzled regulation of Notch signalling polarizes cell fate in the *Drosophila* eye. *Nature* **397**, 526-529.

Dabdoub, A., Donohue, M. J., Brennan, A., Wolf, V., Montcouquiol, M., Sassoon, D. A., Hseih, J. C., Rubin, J. S., Salinas, P. C. and Kelley, M. W. (2003). Wnt signaling mediates reorientation of outer hair cell stereociliary bundles in the mammalian cochlea. *Development* **130**, 2375-2384.

Das, G., Reynolds-Kenneally, J. and Mlodzik, M. (2002). The atypical cadherin Flamingo links Frizzled and Notch signaling in planar polarity establishment in the Drosophila eye. *Dev. Cell* **2**, 655-666.

Das, G., Jenny, A., Klein, T. J., Eaton, S. and Mlodzik, M. (2004). Diego interacts with Prickle and Strabismus/Van Gogh to localize planar cell polarity complexes. *Development* **131**, 4467-4476.
Djiane, A., Yogev, S. and Mlodzik, M. (2005). The apical determinants aPKC and dPatj regulate Frizzled-dependent planar cell polarity in the Drosophila eye. *Cell* **121**, 621-631.
Duchek, P. and Rorth, P. (2001). Guidance of cell migration by EGF receptor signaling during Drosophila oogenesis. *Science* **291**, 131-133.
Duchek, P., Somogyi, K., Jekely, G., Beccari, S. and Rorth, P. (2001). Guidance of cell migration by the Drosophila PDGF/VEGF receptor. *Cell* **107**, 17-26.
Fanto, M. and Mlodzik, M. (1999). Asymmetric Notch activation specifies photoreceptors R3 and R4 and planar polarity in the *Drosophila* eye. *Nature* **397**, 523-526.
Fanto, M., Weber, U., Strutt, D. I. and Mlodzik, M. (2000). Nuclear signaling by Rac and Rho GTPases is required in the establishment of epithelial planar polarity in the Drosophila eye. *Curr. Biol.* **10**, 979-988.
Gaengel, K. and Mlodzik, M. (2003). Egfr signaling regulates ommatidial rotation and cell motility in the Drosophila eye via MAPK/Pnt signaling and the Ras effector Canoe/AF6. *Development* **130**, 5413-5423.
Garcia-Bellido, A., Ripoll, P. and Morata, G. (1976). Developmental compartmentalization in the dorsal mesothoracic disc of Drosophila. *Dev. Biol.* **48**, 132-147.
Hayashi, T. and Carthew, R. W. (2004). Surface mechanics mediate pattern formation in the developing retina. *Nature* **431**, 647-652.
Hazan, R. B., Qiao, R., Keren, R., Badano, I. and Suyama, K. (2004). Cadherin switch in tumor progression. *Ann. N. Y. Acad. Sci.* **1014**, 155-163.
Iwai, Y., Usui, T., Hirano, S., Steward, R., Takeichi, M. and Uemura, T. (1997). Axon patterning requires DN-cadherin, a novel neuronal adhesion receptor, in the Drosophila embryonic CNS. *Neuron* **19**, 77-89.
Klein, T. J. and Mlodzik, M. (2005). Planar cell polarization: an emerging model points in the right direction. *Annu. Rev. Cell Dev. Biol.* **21**, 155-176.
Lee, C. H., Herman, T., Clandinin, T. R., Lee, R. and Zipursky, S. L. (2001). N-cadherin regulates target specificity in the Drosophila visual system. *Neuron* **30**, 437-450.
Lee, M., Lee, S., Zadeh, A. D. and Kolodziej, P. A. (2003). Distinct sites in E-cadherin regulate different steps in Drosophila tracheal tube fusion. *Development* **130**, 5989-5999.
Lu, Z., Ghosh, S., Wang, Z. and Hunter, T. (2003). Downregulation of caveolin-1 function by EGF leads to the loss of E-cadherin, increased transcriptional activity of beta-catenin, and enhanced tumor cell invasion. *Cancer Cell* **4**, 499-515.
Magie, C. R., Pinto-Santini, D. and Parkhurst, S. M. (2002). Rho1 interacts with p120ctn and alpha-catenin, and regulates cadherin-based adherens junction components in Drosophila. *Development* **129**, 3771-3782.
Mlodzik, M. (1999). Planar polarity in the Drosophila eye: a multifaceted view of signaling specificity and cross-talk. *EMBO J.* **18**, 6873-6879.
Mlodzik, M. (2002). Planar cell polarization: do the same mechanisms regulate Drosophila tissue polarity and vertebrate gastrulation? *Trends Genet.* **18**, 564-571.
Montcouquiol, M., Rachel, R. A., Lanford, P. J., Copeland, N. G., Jenkins, N. A. and Kelley, M. W. (2003). Identification of Vangl2 and Scrb1 as planar polarity genes in mammals. *Nature* **423**, 173-177.
Montero, J. A., Carvalho, L., Wilsch-Brauninger, M., Kilian, B., Mustafa, C. and Heisenberg, C. P. (2005). Shield formation at the onset of zebrafish gastrulation. *Development* **132**, 1187-1198.
Naora, H. and Montell, D. J. (2005). Ovarian cancer metastasis: integrating insights from disparate model organisms. *Nat. Rev. Cancer* **5**, 355-366.
Newsome, T. P., Asling, B. and Dickson, B. J. (2000). Analysis of Drosophila photoreceptor axon guidance in eye-specific mosaics. *Development* **127**, 851-860.
Niewiadomska, P., Godt, D. and Tepass, U. (1999). DE-Cadherin is required for intercellular motility during Drosophila oogenesis. *J. Cell Biol.* **144**, 533-547.
Oda, H. and Tsukita, S. (1999). Nonchordate classic cadherins have a structurally and functionally unique domain that is absent from chordate classic cadherins. *Dev. Biol.* **216**, 406-422.
Oda, H., Tsukita, S. and Takeichi, M. (1998). Dynamic behavior of the cadherin-based cell-cell adhesion system during Drosophila gastrulation. *Dev. Biol.* **203**, 435-450.
Orsulic, S. and Peifer, M. (1996). An in vivo structure-function study of armadillo, the beta-catenin homologue, reveals both separate and overlapping regions of the protein required for cell adhesion and for wingless signaling. *J. Cell Biol.* **134**, 1283-1300.
Pacquelet, A., Lin, L. and Rorth, P. (2003). Binding site for p120/delta-catenin is not required for Drosophila E-cadherin function in vivo. *J. Cell Biol.* **160**, 313-319.
Perez-Moreno, M., Jamora, C. and Fuchs, E. (2003). Sticky business: orchestrating cellular signals at adherens junctions. *Cell* **112**, 535-548.
Pignoni, F. and Zipursky, S. L. (1997). Induction of Drosophila eye development by decapentaplegic. *Development* **124**, 271-278.
Prakash, S., Caldwell, J. C., Eberl, D. F. and Clandinin, T. R. (2005). Drosophila N-cadherin mediates an attractive interaction between photoreceptor axons and their targets. *Nat. Neurosci.* **8**, 443-450.
Sanson, B., White, P. and Vincent, J. P. (1996). Uncoupling cadherin-based adhesion from wingless signalling in Drosophila. *Nature* **383**, 627-630.
Shulman, J. M., Perrimon, N. and Axelrod, J. D. (1998). Frizzled signaling and the developmental control of cell polarity. *Trends Genet.* **14**, 452-458.
St Johnston, D. (2002). The art and design of genetic screens: Drosophila melanogaster. *Nat. Rev. Genet.* **3**, 176-188.
Strutt, D. I., Weber, U. and Mlodzik, M. (1997). The role of RhoA in tissue polarity and Frizzled signalling. *Nature* **387**, 292-295.
Strutt, H. and Strutt, D. (1999). Polarity determination in the Drosophila eye. *Curr. Opin. Genet. Dev.* **9**, 442-446.
Strutt, H. and Strutt, D. (2003). EGF signaling and ommatidial rotation in the Drosophila eye. *Curr. Biol.* **13**, 1451-1457.
Tanentzapf, G., Smith, C., McGlade, J. and Tepass, U. (2000). Apical, lateral, and basal polarization cues contribute to the development of the follicular epithelium during Drosophila oogenesis. *J. Cell Biol.* **151**, 891-904.
Tepass, U., Gruszynski-DeFeo, E., Haag, T. A., Omatyar, L., Torok, T. and Hartenstein, V. (1996). shotgun encodes Drosophila E-cadherin and is preferentially required during cell rearrangement in the neurectoderm and other morphogenetically active epithelia. *Genes Dev.* **10**, 672-685.
Tepass, U., Truong, K., Godt, D., Ikura, M. and Peifer, M. (2000). Cadherins in embryonic and neural morphogenesis. *Nat. Rev. Mol. Cell Biol.* **1**, 91-100.
Tomlinson, A. and Struhl, G. (1999). Decoding vectorial information from a gradient: sequential roles of the receptors Frizzled and Notch in establishing planar polarity in the Drosophila eye. *Development* **126**, 5725-5738.
Tomlinson, A., Bowtell, D. D., Hafen, E. and Rubin, G. M. (1987). Localization of the sevenless protein, a putative receptor for positional information, in the eye imaginal disc of Drosophila. *Cell* **51**, 143-150.
Uemura, T., Oda, H., Kraut, R., Hayashi, S., Kotaoka, Y. and Takeichi, M. (1996). Zygotic Drosophila E-cadherin expression is required for processes of dynamic epithelial cell rearrangement in the Drosophila embryo. *Genes Dev.* **10**, 659-671.
Veeman, M. T., Axelrod, J. D. and Moon, R. T. (2003). A second canon. Functions and mechanisms of beta-catenin-independent Wnt signaling. *Dev. Cell* **5**, 367-377.
Weber, U., Eroglu, C. and Mlodzik, M. (2003). Phospholipid membrane composition affects EGF receptor and Notch signaling through effects on endocytosis during Drosophila development. *Dev. Cell* **5**, 559-570.
Winter, C. G., Wang, B., Ballew, A., Royou, A., Karess, R., Axelrod, J. D. and Luo, L. (2001). Drosophila Rho-associated kinase (Drok) links Frizzled-mediated planar cell polarity signaling to the actin cytoskeleton. *Cell* **105**, 81-91.
Wolff, T. and Ready, D. F. (1993). Pattern formation in the *Drosophila* retina. In *The Development of Drosophila melanogaster* (ed. M. B. A. Martinez-Arias), pp. 1277-1326. Cold Spring Harbor: Cold Spring Harbor Press.
Wu, J., Klein, T. J. and Mlodzik, M. (2004). Subcellular localization of frizzled receptors, mediated by their cytoplasmic tails, regulates signaling pathway specificity. *PLoS Biol.* **2**, E158.
Yanagawa, S., Lee, J. S., Haruna, T., Oda, H., Uemura, T., Takeichi, M. and Ishimoto, A. (1997). Accumulation of Armadillo induced by Wingless, Dishevelled, and dominant-negative Zeste-White 3 leads to elevated DE-cadherin in Drosophila clone 8 wing disc cells. *J. Biol. Chem.* **272**, 25243-25251.
Yap, A. S. and Kovacs, E. M. (2003). Direct cadherin-activated cell signaling: a view from the plasma membrane. *J. Cell Biol.* **160**, 11-16.
Yeaman, C., Grindstaff, K. K. and Nelson, W. J. (1999). New perspectives on mechanisms involved in generating epithelial cell polarity. *Physiol. Rev.* **79**, 73-98.